J|A|C|S
ARTICLES

Published on Web 10/25/2010

Saturation of Surfactant Structure at the Single-Walled Carbon Nanotube Surface

Juan G. Duque,[†] Crystal G. Densmore,[‡] and Stephen K. Doorn*[,§]

Chemistry Division, Physical Chemistry and Applied Spectroscopy Group (C-PCS), and Chemical Diagnostics and Engineering Group (C-CDE), and Materials Physics and Applications Division, Center for Integrated Nanotechnologies (MPA-CINT), Los Alamos National Laboratory, Los Alamos, New Mexico 87545, United States

Received July 30, 2010; E-mail: skdoorn@lanl.gov

Abstract: Density gradient ultracentrifugation (DGU) and fluorescence spectroscopy are used to probe the limiting behaviors of the dynamic response of surfactant structure at the single-walled carbon nanotube (SWNT) surface to reorganizing forces, including changes in surfactant concentration and electrolyte screening. DGU results indicate that, as surfactant (sodium dodecyl sulfate, SDS) concentration is increased, SDS adsorbed on metallic SWNTs becomes limited in its ability to reorganize before SDS adsorbed on semiconducting species. A diameter-dependent enhancement is observed in photoluminescence intensities from semiconducting SWNTS upon initial titration with NaCl. This response to electrostatic screening diminishes as SDS concentration is increased. The results are understood as a saturation of the surfactant structural response, defined as both a loss in ability to increase SDS loading at the SWNT surface and a loss in ability to reorient surface structure in response to a reorganizing force. Saturation of response is found to be reversible and also occurs as a result of restricting SDS mobility. These results confirm several aspects of recent molecular dynamics simulations of SDS behavior on SWNTs and have important implications for tunability of density-based separation approaches using cosurfactant systems that include SDS.

Introduction

The fundamental behaviors of low-dimensional nanomaterials are highly sensitive to the effects of changing surface environment, surface doping, and functionalization chemistry, due to the high percentage of their constituent atoms residing at the surface. For example, electron transport and optical response in semiconducting nanowires are highly tunable through surface control of trap states and doping levels.[1−3] A detailed understanding of surface chemistry is also critical to rationally modifying optical responses, as was recently demonstrated in the ability to stabilize emission from quantum dots through appropriate surface functionalization.[4] Sensitivity to surface environment is especially true in single-walled carbon nanotubes (SWNTs), whose entire structure consists of surface atoms. Of particular interest is the response of the unique photophysical properties of SWNTs, especially the near-infrared emission of semiconducting species,[5,6] to surface interactions and changes in the local environment.

The ability to generate stable solution suspensions of SWNTs through noncovalent surface functionalization with surfactants[5] has played a central role in revealing their optical and electronic properties. Furthermore, modification of surfactant properties and their surface interactions provides a ready means to tune the SWNT optical response. For instance, the excitonic nature of the SWNT electronic transitions[7−9] makes it possible to alter their optical response through tuning of the dielectric environment in which they are studied. This can shift their electronic transitions and alter exciton binding energies.[9−12] Such environmental effects can be significantly modulated by surfactant

[†] C-PCS.
[‡] C-CDE.
[§] MPA-CINT.

(1) Leonard, F.; Talin, A. A.; Swartzentruber, B. S.; Picraux, S. T. *Phys. Rev. Lett.* **2009**, *102*, 106805.
(2) Kelzenberg, M. D.; Turner-Evans, D. B.; Kayes, B. M.; Filler, M. A.; Putnam, M. C.; Lewis, N. S.; Atwater, H. A. *Nano Lett.* **2008**, *8*, 710–714.
(3) Perea, D. E.; Hemesath, E. R.; Schwalbach, E. J.; Lensch-Falk, J. L.; Voorhees, P. W.; Lauhon, L. J. *Nat. Nanotechnol.* **2009**, *4*, 315–319.
(4) Chen, Y.; Vela, J.; Htoon, H.; Casson, J. L.; Werder, D. J.; Bussian, D. A.; Klimov, V. I.; Hollingsworth, J. A. *J. Am. Chem. Soc.* **2008**, *130*, 5026–5027.
(5) O'Connell, M. J.; Bachilo, S. M.; Huffman, C. B.; Moore, V. C.; Strano, M. S.; Haroz, E. H.; Rialon, K. L.; Boul, P. J.; Noon, W. H.; Kittrell, C.; Ma, J.; Hauge, R. H.; Weisman, R. B.; Smalley, R. E. *Science* **2002**, *297*, 593–596.
(6) Bachilo, S. M.; Strano, M. S.; Kittrell, C.; Hauge, R. H.; Smalley, R. E.; Weisman, R. B. *Science* **2002**, *298*, 2361–2366.
(7) Wang, F.; Dukovic, G.; Brus, L. E.; Heinz, T. F. *Science* **2005**, *308*, 838–841.
(8) Spataru, C. D.; Ismail-Beigi, S.; Benedict, L. X.; Louie, S. G. *Phys. Rev. Lett.* **2004**, *92*, 077402.
(9) Perebeinos, V.; Tersoff, J.; Avouris, P. *Phys. Rev. Lett.* **2004**, *92*, 257402.
(10) Walsh, A. G.; Vamivakas, A. N.; Yin, Y.; Cronin, S. B.; Unlu, M. S.; Goldberg, B. B.; Swan, A. K. *Nano Lett.* **2007**, *7*, 1485–1488.
(11) Araujo, P. T.; Jorio, A.; Dresselhaus, M. S.; Sato, K.; Saito, R. *Phys. Rev. Lett.* **2009**, *103*, 146802.
(12) Miyauchi, Y.; Saito, R.; Sato, S.; Ohno, Y.; Iwasaki, S.; Mizutani, T.; Jiang, J.; Maruyama, S. *Chem. Phys. Lett.* **2007**, *442*, 394–399.

concentration and molecular structure.[13−18] These in part define the surfactant interaction and conformation at the SWNT surface, which can be further tuned by external factors such as shear forces,[19] temperature,[20] and ionic strength.[20,21] Moreover, specific chemical interactions with species including protons,[22−24] water,[13] and other molecules[23,25−27] can be mediated by the surfactant. Recently, it has been demonstrated that surfactant conformation and structure play an important role in the chemical reactivity of suspended SWNTs by limiting access to the SWNT surface.[23,27−29] Ultimately, these extrinsic factors will impact spectral line-widths, exciton dynamics, and emission quantum yields,[7,18,28,30−32] having pronounced implications for sensing, imaging, nanophotonics, and optoelectronics applications.[33−36]

In addition to the important role played by surfactants in determining SWNT photophysical properties, the structural dependence of their interactions with the SWNT surface is also key in new approaches to SWNT separation according to chirality or type via density gradient ultracentrifugation (DGU).[37,38] Complex cosurfactant systems used in DGU enable separation by changing the effective SWNT buoyancy in a manner sensitive to the underlying SWNT structure, allowing the different structures to fractionate into their respective isopycnic points within the density gradient.[38,39] Surfactant−nanotube interactions depend on SWNT structure,[20,40,41] supporting the suggestion that the composition and diameter-dependent competitive binding interactions in cosurfactant systems are the driving mechanisms behind SWNT separation.[38,39,42−45] Recently, a single surfactant approach involving SWNT suspensions in sodium dodecylsulfate (SDS) modified by NaCl addition was reported to obtain type and diameter separated SWNTs.[21] Niyogi et al. suggested a model for this single surfactant process that involves the reorganization of the SDS molecules adsorbed on the SWNT surface via screening of electrostatic interactions. The result is an effective change in the SWNT/surfactant composite volume that amplifies diameter-dependent density differences.[21]

Despite the critical role surfactants play in determining a broad range of nanotube optical, physical, and chemical behavior, the detailed nature of surfactant interaction and structure at the nanotube surface is not yet well understood. Emerging experimental[19−21,26,46] and theoretical reports[47−52] on SDS dispersed SWNTs suggest that the surfactant structure is dynamic, with multiple regimes of tunability that can be invoked for optical and separation applications. Recent molecular dynamics (MD) simulations indicate that surfactant concentration and SWNT diameter and chiral structure all affect the resulting micelle structure around the SWNTs.[47−52] It has also been demonstrated that initial surfactant conformations can be further manipulated by physical and chemical influences.[19−21,27] However, to utilize surfactant structure as a more effective tunable parameter for designing photophysical and chemical response and for enhancing separations, several fundamental questions related to these dynamic behaviors must be addressed. Among these are the need to understand the limits of attainable reorganization of surfactant conformation and micelle structure and how the tunability of these surface structures is constrained by SWNT chirality. It is also important to understand if similar limits apply generally to all surfactants.

In this work, we probe the limits of the dynamic tunability of surfactant structures at the SWNT surface and provide important experimental support for several features emerging from the recent MD modeling studies. Our focus is on optical

(13) Moore, V. C.; Strano, M. S.; Haroz, E. H.; Hauge, R. H.; Smalley, R. E. *Nano Lett.* **2003**, *3*, 1379–1382.
(14) Tan, Y.; Resasco, D. E. *J. Phys. Chem. B* **2005**, *109*, 14454–14460.
(15) Wenseleers, W.; Vlasov, I. I.; Goovaerts, E.; Obraztsova, E. D.; Lobach, A. S.; Bouwen, A. *Adv. Funct. Mater.* **2004**, *14*, 1105–1112.
(16) Ishibashi, A.; Nakashima, N. *Chem.-Eur. J.* **2006**, *12*, 7595–7602.
(17) Fantini, C.; Cassimiro, J.; Peressinotto, V. S. T.; Plentz, F.; Souza Filho, A. G.; Furtado, C. A.; Santos, A. P. *Chem. Phys. Lett.* **2009**, *473*, 96–101.
(18) Duque, J. G.; Pasquali, M.; Cognet, L.; Lounis, B. *ACS Nano* **2009**, *3*, 2153–2156.
(19) Silvera-Batista, C. A.; Weinberg, P.; Butler, J. E.; Ziegler, K. J. *J. Am. Chem. Soc.* **2009**, *131*, 12721–12728.
(20) Niyogi, S.; Boukhalfa, S.; Chikkannanavar, S. B.; McDonald, T. J.; Heben, M. J.; Doorn, S. K. *J. Am. Chem. Soc.* **2007**, *129*, 1898–1899.
(21) Niyogi, S.; Densmore, C. G.; Doorn, S. K. *J. Am. Chem. Soc.* **2009**, *131*, 1144–1153.
(22) Strano, M. S.; Huffman, C. B.; Moore, V. C.; O'Connell, M. J.; Haroz, E. H.; Hubbard, J.; Miller, M.; Rialon, K.; Kittrell, C.; Ramesh, S.; Hauge, R. H.; Smalley, R. E. *J. Phys. Chem. B* **2003**, *107*, 6979–6985.
(23) Duque, J. G.; Cognet, L.; Parra-Vasquez, A. N. G.; Nicholas, N.; Schmidt, H. K.; Pasquali, M. *J. Am. Chem. Soc.* **2008**, *130*, 2626–2633.
(24) Cognet, L.; Tsyboulski, D. A.; Rocha, J.-D. R.; Doyle, C. D.; Tour, J. M.; Weisman, R. B. *Science* **2007**, *316*, 1465–1468.
(25) O'Connell, M. J.; Eibergen, E. E.; Doorn, S. K. *Nat. Mater.* **2005**, *4*, 412–418.
(26) Wang, R. K.; Chen, W.-C.; Campos, D. K.; Ziegler, K. J. *J. Am. Chem. Soc.* **2008**, *130*, 16330–16337.
(27) Chen, W.-C.; Wang, R. K.; Ziegler, K. J. *ACS Appl. Mater. Interfaces* **2009**, *1*, 1821–1826.
(28) Ju, S.-Y.; Kopcha, W. P.; Papadimitrakopoulos, F. *Science* **2009**, *323*, 1319–1323.
(29) Wang, R.; Cherukuri, P.; Duque, J. G.; Leeuw, T. K.; Lackey, M. K.; Moran, C. H.; Moore, V. C.; Conyers, J. L.; Smalley, R. E.; Schmidt, H. K.; Weisman, R. B.; Engel, P. S. *Carbon* **2007**, *45*, 2388–2393.
(30) Jones, M.; Engtrakul, C.; Metzger, W. K.; Ellingson, R. J.; Nozik, A. J.; Heben, M. J.; Rumbles, G. *Phys. Rev. B* **2005**, *71*, 115426.
(31) Berger, S.; Voisin, C.; Cassabois, G.; Delalande, C.; Roussignol, P.; Marie, X. *Nano Lett.* **2007**, *7*, 398–402.
(32) Tsyboulski, D. A.; Bakota, E. L.; Witus, L. S.; Rocha, J.-D. R.; Hartgerink, J. D.; Weisman, R. B. *J. Am. Chem. Soc.* **2008**, *130*, 17134–17140.
(33) Barone, P. W.; Baik, S.; Heller, D. A.; Strano, M. S. *Nat. Mater.* **2005**, *4*, 86–92.
(34) Satishkumar, B. C.; Brown, L. O.; Gao, Y.; Wang, C.-C.; Wang, H.-L.; Doorn, S. K. *Nat. Nanotechnol.* **2007**, *2*, 560–564.
(35) Kim, J.-H.; Heller, D. A.; Jin, H.; Barone, P. W.; Song, C.; Zhang, J.; Trudel, L. J.; Wogan, G. N.; Tannenbaum, S. R.; Strano, M. S. *Nat. Chem.* **2009**, *1*, 473–481.
(36) Misewich, J. A.; Martel, R.; Avouris, Ph.; Tsang, J. C.; Heinze, S.; Tersoff, J. *Science* **2003**, *300*, 783–786.
(37) Arnold, M. S.; Stupp, S. I.; Hersam, M. C. *Nano Lett.* **2005**, *5*, 713–718.
(38) Arnold, M. S.; Green, A. A.; Hulvat, J. F.; Stupp, S. I.; Hersam, M. C. *Nat. Nanotechnol.* **2006**, *1*, 60–65.
(39) Yanagi, K.; Miyata, Y.; Kataura, H. *Appl. Phys. Express* **2008**, *1*, 034003.
(40) McDonald, T. J.; Engtrakul, C.; Jones, M.; Rumbles, G.; Heben, M. J. *J. Phys. Chem. B* **2006**, *110*, 25339–25346.
(41) Duque, J. G.; et al. *ACS Nano* **2010**, *4*, 3063–3072.
(42) Hersam, M. C. *Nat. Nanotechnol.* **2008**, *3*, 387–394.
(43) Green, A. A.; Hersam, M. C. *Nano Lett.* **2008**, *8*, 1417–1422.
(44) Miyata, Y.; Yanagi, K.; Maniwa, Y.; Kataura, H. *J. Phys. Chem. C* **2008**, *112*, 3591–3596.
(45) Ju, S. Y.; Doll, J.; Sharma, I.; Papadimitrakopoulos, F. *Nat. Nanotechnol.* **2008**, *3*, 356–362.
(46) Wang, H. *Curr. Opin. Colloid Interface Sci.* **2009**, *14*, 364–371.
(47) Wallace, E. J.; Sansom, M. S. P. *Nano Lett.* **2007**, *7*, 1923–1928.
(48) Calvaresi, M.; Dallavalle, M.; Zerbetto, F. *Small* **2009**, *5*, 2191–2198.
(49) Tummala, N. R.; Striolo, A. *ACS Nano* **2009**, *3*, 595–602.
(50) Tummala, N. R.; Striolo, A. *Phys. Rev. E* **2009**, *80*, 021408.
(51) Angelikopoulos, P.; Gromov, A.; Leen, A.; Nerushev, O.; Bock, H.; Campbell, E. E. B. *J. Phys. Chem. C* **2010**, *114*, 2–9.
(52) Xu, Z.; Yang, X.; Yang, Z. *Nano Lett.* **2010**, *10*, 985–991.

studies that serve as a probe for understanding how surfactant structure at the nanotube surface changes in response to environmental perturbations. We demonstrate that, as SDS concentration in solution is increased, the ability of the nanotube surface to absorb an increased surfactant loading and the ability for the SDS surface structures to reorganize in response to electrostatic screening become saturated. The results of DGU separations at different SDS loadings motivate our optical studies by demonstrating that surfactant structures at metallic SWNT surfaces become saturated earlier than the corresponding semiconducting species. Optical probing of electrolyte-induced surfactant reorganization at semiconducting surfaces indicates a similar structural saturation at sufficiently high SDS concentrations. While saturation behaviors are found to have a significant diameter dependence, we demonstrate the primary signatures of saturation are a general behavior across all diameters and chirality. The importance of surfactant reorientation as a factor in the observed saturation behavior is underscored by the ability to restrict SDS mobility by fixing its surface orientation with a polymer layer. Similarly, the restricted ability of close-packed, strongly interacting surfactants such as deoxycholate to respond to varying electrostatic environments indicates that the saturation behavior of SDS is not general to all surfactants. We find these results to support our model of the SDS−nanotube interaction as a dynamic and highly tunable composite structure with implications for further controlling photophysical behavior and enhancing density-based separations.[21]

Experimental Section

SWNT Dispersions. HiPco SWNTs (Rice University) were individualized by dispersing them with standard suspension procedures[5] as follows. Ten milligrams of raw HiPco (batch 189.2 and 120.5, with mean diameters of 0.78 and 1.0 nm, respectively; see the Supporting Information) SWNTs was dispersed in 30 mL of D_2O using dodecylbenzenesulfonic acid, sodium salt (SDBS), sodium dodecylsulfate (SDS), or sodium deoxycholate (DOC) at 0.5, 1.0, 1.5, and 2.0 wt % (wt%) surfactant concentration. The suspension procedures were slightly modified from previous reports to minimize the formation of side-wall defects so that highly luminescent SWNTs could be obtained. Homogenization was done at 19 000 rpm (X520 CAT or PowerGen 700D shear mixer) for 10 min, followed by tip sonication at 20−25 W for 8 min in a cold water bath (Cole Parmer CPX 750). Sonication time and power were kept low to minimize SWNT cutting and sidewall defects. The sample was then ultracentrifuged at 29 000 rpm (∼144 000*g*) for 4 h in a Beckmann-Coulter TH-641 swing bucket rotor in a Sorvall WX Ultra 80 centrifuge. Contamination of the supernatant with nanotube bundles was minimized by collecting only the top 70% of the supernatant. For spectral analysis, the concentration of the SWNT suspensions was adjusted to roughly 10 mg/L by UV−vis−nIR.[53]

SDS−Poly(vinyl pyrrolidone) (SDS−PVP) SWNT Suspensions. SDS−PVP SWNT suspensions were prepared following procedures published elsewhere[23] by mixing three-parts SDS surfactant-suspended SWNTs and one-part 55 000 molecular weight poly(vinyl pyrrolidone) (PVP) solution. The concentration was adjusted to give a final concentration of roughly 0.75 wt % SDS−SWNTs and 0.25 wt % PVP.

Salt Titration. Aliquots of aqueous NaCl (1 M) solution were added to 500 μL of surfactant stabilized SWNTs (HiPco batch 189.2) and mixed thoroughly with a vortex mixer. After each addition of salt, spectral characterization was conducted. To verify that the volume of salt solution added to the SWNT suspension did not affect the emission intensity by simple dilution, identical aliquots of D_2O were added to a separate suspension for direct comparison (see the Supporting Information).

Density Gradient Ultracentrifugation (DGU) Separation. HiPco (batch 120.5) suspensions were prepared with three different initial surfactant concentrations, 1.25, 1.50, and 2.0 wt %. Suspension preparation and DGU separation of the resulting SDS-SWNT suspensions were conducted using previously published procedures.[21] The density gradient column was formed from manually layering aqueous dilutions of a commercially available 60 weight by volume percent ((w/v)%) aqueous solution of iodixanol (OptiPrep density gradient medium, Aldrich Chemical Co.). Aqueous dilutions of iodixanol were prepared with 2 (w/v)% SDS in DI water to give 20 (w/v)%, 30 (w/v)%, and 40 (w/v)% iodixanol solutions. The density gradient column was formed in Beckman 3 mL capacity thick-wall polyallomer tubes by carefully layering 200 μL 60 (w/v)%, 500 μL 40 (w/v)%, 500 μL 30 (w/v)%, and then 300 μL 20 (w/v)% at the top. The column was allowed to diffuse for 1 h at room temperature at an angle of approximately 20° from the vertical. Following formation of the density gradient column, 50 μL of 1 M (aq) NaCl was added to 500 μL of the SDS−SWNT dispersion to give a final concentration of 91 mM NaCl. The suspension was stirred for 10−15 min at 800−1000 rpm. The NaCl−SDS−SWNT dispersion (550 μL total) was carefully injected above the 20 (w/v)% iodixanol layer using a syringe. The samples were then centrifuged at 25 °C for 6 h at 49 000 rpm (∼250 000*g*) using a Beckman Coulter SW60Ti swing bucket rotor in a Sorvall WX Ultra 80 centrifuge.

Spectroscopic Characterization. Photoluminescence excitation (PLE) maps, fluorescence, and absorbance spectra were obtained from solutions adjusted to roughly the same SWNT concentration. All optical spectra were normalized to concentration. Absorbance spectra were recorded on a Varian Cary 6000i instrument. Emission spectra were obtained with excitation wavelengths between 450 and 800 nm using a xenon lamp coupled to a monochromator system with 10 nm band-pass and 5 nm excitation steps. The emission intensities were recorded between 900 and 1600 nm using a modified Nicolet NXR-9600 FT-IR spectrometer equipped with a liquid-N_2 cooled germanium detector.[25] Spectra were obtained as averages of 100 scans, with a spectral resolution of 16 cm^{-1}. SWNT fluorescence spectra were also obtained with single line excitation using a 780 nm diode laser at 20 mW incident power.

Results and Discussion

Surfactant Concentration Effects on Electrolyte-Mediated DGU Separations: Saturation of Metallic Surface Structures. Recently, we demonstrated that, by tuning the SDS/SWNT interfacial dynamics through addition of electrolyte, diameter-dependent separation of metallic and semiconducting SWNTs can be achieved with density gradient ultracentrifugation, without the use of an additional cosurfactant.[21] A model for the process suggests that electrolyte screening results in an increased SDS packing density that in effect arises from a decrease in the critical micelle concentration (cmc) as electrolyte is added. The typical SDS cmc of 8.3 mM drops to 5.2 mM in 0.01 M Na^+, and to 1.5 mM in 0.10 M Na^+.[54] Hayashi and Ikeda further show that, as the cmc decreases, the aggregation number of SDS molecules in a micelle increases.[54] The same is expected to occur for the SDS assemblies at the SWNT surface, where the increase in aggregation number induces a change in the surfactant orientation at the SWNT interface to a more ordered perpendicular structure with polar headgroups extended more uniformly away from the SWNT surface. The result is an effective increase in the surfactant volume fraction

(53) Attal, S.; Thiruvengadathan, R.; Regev, O. *Anal. Chem.* **2006**, *78*, 8098–8104.

(54) Hayashi, S.; Ikeda, S. *J. Phys. Chem. B* **1980**, *84*, 744–751.

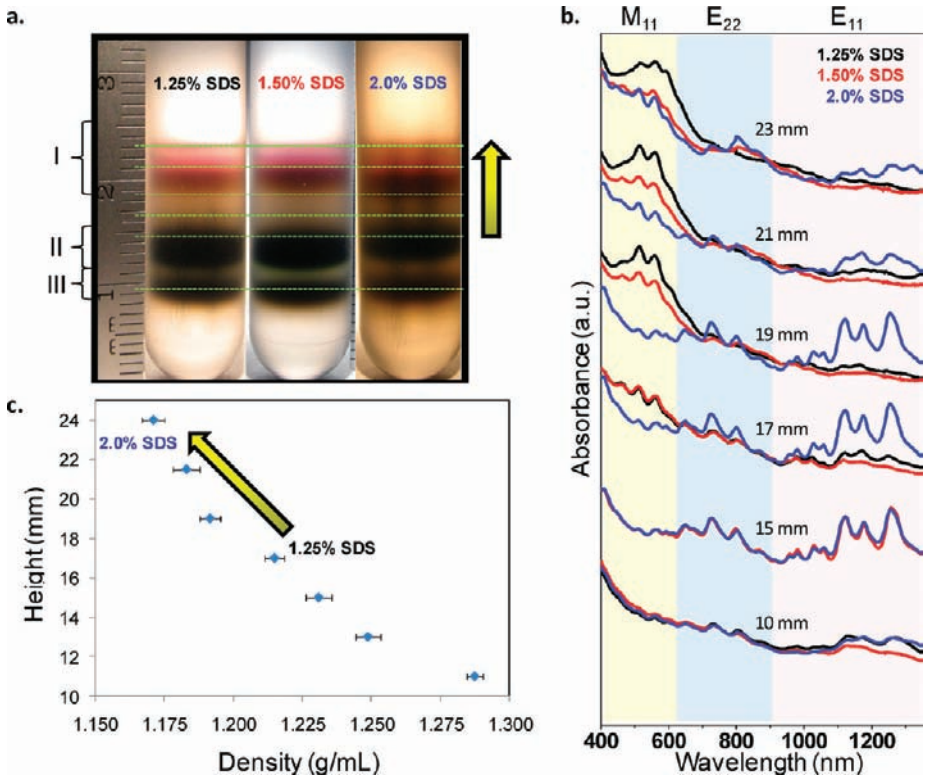

Figure 1. (a) Images of three centrifuge tubes after DGU with 1.25%, 1.50%, and 2.0% SDS dispersions (HiPco batch 120.5) with 91 mM added NaCl. The green dotted lines represent the SWNT fractions that were extracted for absorbance measurements. (b) Absorbance spectra of the fractions indicated by the green dashed lines in (a). The yellow, blue, and pink boxes highlight the M_{11}, E_{22}, and E_{11} transitions of metallic and semiconducting SWNTs, respectively. All spectra are normalized to absorbance at 764 nm. (c) Height in tube (mm) versus density (g/mL). Density trend of highest semiconductor fraction is noted for 1.25% and 2% SDS and is highlighted with yellow arrow.

around the SWNTs that amplifies the diameter-dependent density differences of different SWNT structures, thus enabling SWNT separation.[21] As noted in ref 21, the process of surfactant reorientation is enhanced on metallic SWNTs as a result of the formation of an image charge upon SDS adsorption. The image charge serves to screen SDS headgroup interactions further, allowing a greater degree of SDS packing to occur in comparison to semiconducting structures (in 1.25 wt % SDS). Typical separation results are shown in Figure 1a. Centrifuged samples prepared with 1.25 wt % SDS and 91 mM added NaCl show three visibly distinct bands (denoted by I, II, and III, Figure 1a), attributed to enriched metallic, semiconductor, and bundled fractions, respectively.[21] The black traces at heights of 19−23 mm in Figure 1b show the absorbance spectra obtained for the metallic region. The predominant peaks are in the region associated with the M_{11} transitions for metallic SWNTs (m-SWNTs), with little contribution observed from the E_{11} or E_{22} transitions for the semiconducting SWNTs (s-SWNTs).[5] At 1.25% SDS levels, spectra begin to show the presence of s-SWNTs beginning at 17 mm and lower in the tube.

Performing a similar separation at increased surfactant concentrations (1.5 wt % and 2 wt % SDS, with same salt concentration) results in several interesting changes to the relative fractionation behavior of metallic and semiconducting SWNTs. As seen in Figure 1a (center and right tubes), the metallic fractions in the 1.5 wt % and 2 wt % cases remain at the identical isopycnic points as found in 1.25% SDS (region I). The enriched semiconducting fractions (region II), however, now migrate to lower density regions higher in the tube. This observation is evident by the color change observed in Figure 1a and noted by the accompanying arrow. The metallic region I changes from light pink to a dark red at around 20 mm in height, and the discrete separation between the metallic and semiconducting regions becomes blurred as SDS concentration is increased. The decrease in semiconducting densities associated with migration higher in the tube is further evidenced by the observed changes in the absorption spectra of region I. The absorbance spectra at heights of 19, 21, and 23 mm for the 1.5% and 2% SDS cases (Figure 1b, red and blue traces, respectively) now clearly show features from the semiconducting E_{11} and E_{22} peaks, as well as E_{33} features occurring in the shorter wavelength region previously dominated by metallic M_{11} features. Furthermore, these features progressively strengthen and rise to higher levels on going from 1.25% to 1.5% and finally 2.0% SDS. Because spectra are normalized to the absorbance at 764 nm in the s-SWNT E_{22} region, the progressive loss in relative M_{11} absorbance as SDS concentration is increased is also indicative of semiconducting species rising higher in the tube (and does not indicate an overall loss of metallic species in these locations).

The contrasting behavior of the metallic and semiconducting fractions under the influence of an increased SDS level can be understood by returning to our simple model. In general, as SDS concentration increases, aggregation number in the micelles also increases.[55] While quantitative behavior may differ between aggregation numbers in the micelle versus at the SWNT surface, higher SDS concentrations are therefore expected to lead to a further increase in SDS packing density. The result is a continued reorientation of SDS structure at the nanotube surface, going from disordered SDS lying along the SWNT surface

(55) Benrraou, M.; Bales, B. L.; Zana, R. *J. Phys. Chem. B* **2003**, *107*, 13432–13440.

transforming to more ordered structures with SDS aligned perpendicular to the surface. The consequent increase in volume of the composite structure leads to a corresponding decrease in overall density of the SDS/SWNT composite structure. This is illustrated in Figure 1c with the topmost semiconducting species moving in a continuous progression to lower densities (higher in the tube) as SDS levels are increased. The lack of movement of the metal fractions, however, indicates the packing density of SDS and the ability of its surface structure to further respond to such external perturbations has already become saturated at 1.25% SDS concentrations, in the presence of the added NaCl. The further decrease in semiconducting densities under the same conditions indicates their surfactant structure is still able to respond to external influences and has not yet become saturated. The higher concentration of free surfactant in the system drives more SDS onto the s-SWNT surface, where the surfactant structure is still free to reorganize, ultimately leading to the observed higher volume fractions and lower densities.

We note our model differs from that proposed by Moshammer et al.,[56] whose results suggest the ability to separate metallic from semiconducting nanotubes in SDS suspensions is due to semiconducting SWNTs existing primarily as high density bundles and metallic SWNTs being present as low density individuals.[56] There is no inherent conflict between the models, however, because the difference in mechanism can be understood as resulting from the different diameter distributions present in our respective samples. The work of ref 56 used pulsed laser vaporization-produced SWNTS comprised of larger diameter nanotubes (~1.2−1.5 nm). These larger diameter SWNTs are known to be more difficult to disperse[41] and are therefore more likely to exist in bundles. The significantly smaller diameters (0.78 and 1.0 nm mean diameters) present in our HiPco source material (batches 189.2 and 120.5) are more efficiently dispersed as individuals (see also the Supporting Information). As individuals, the densities of the SWNT/SDS composites will therefore be more susceptible to tuning via SDS reorientation. Furthermore, the principles of surfactant behavior described here will be just as valid at the surface of bundles as they are for individuals.

Our results and interpretation are also consistent with several recent molecular dynamics (MD) simulations of surfactant−SWNT interactions, which suggest that surfactant concentration and composition will affect the dynamics and conformation of the surfactant molecules around the SWNT.[47−52] While current capability does not allow these simulations to discriminate between the behavior of metallic and semiconducting SWNTs, they suggest a number of behaviors general to both types that are supported by our results. For instance, at low surfactant concentration, the surface coverage is described as consisting of more randomly oriented or agglomerated structures along the SWNT axis. At high surfactant concentrations, an increased degree of organization appears in the simulations, resulting from a more uniform and densely packed coverage that acts to project surfactant headgroups perpendicularly away from the SWNT surface and more directly into the surrounding solvent. Coverage is also shown to approach saturation at higher surfactant concentrations.[48,49] The MD results are consistent with our picture that an increased packing density acts to reorient the surfactant structure to generate a higher volume composite structure. Although our separation results using 1.25 and 2 wt % SDS suspensions clearly establish that m-SWNTs undergo surfactant saturation, it is important to determine if similar behavior extends to semiconducting species. The photoluminescence response of the SWNT suspensions has been demonstrated as a sensitive probe of surfactant structure and dynamics at the SWNT surface.[21] Semiconductors will therefore provide a convenient system on which to further investigate surfactant saturation behavior optically.

Optical Studies of Surfactant Saturation in Semiconducting Nanotubes (s-SWNTs). As discussed above, electrolyte screening acts as a reorganizing force on the SDS interfacial behavior at the SWNT surface. The progression in surfactant structural changes that occurs as electrolyte concentration is increased may be tracked through corresponding changes in the photoluminescence (PL) spectra of semiconducting nanotubes (s-SWNTs). We have previously shown that as SDS reorients and packing density increases in response to increased screening, a simultaneous increase in PL intensities, along with spectral narrowing and blue shifting (by ~3 nm), is observed up to some threshold. Once the electrolyte concentration becomes too high, selective diameter-dependent aggregation abruptly bleaches the SWNT emission.[20,21] This behavior was established for moderate-to-large diameter tubes (d > 0.9 nm), but could not be probed sensitively at small diameters due to their low levels in that particular sample (mean d of ~1 nm). With its diameter distribution shifted to much smaller species (mean d of ~0.78 nm),[41] our current sample (HiPco 189.2) allows us to now generalize this behavior to much smaller diameter structures.

Figure 2a−e shows the typical spectroscopic behavior of s-SWNTs as NaCl is added to SWNT suspensions prepared with HiPco 189.2 in 1 wt % SDS and serves the important function of connecting the behavior of the large diameter species of our previous study[21] to that of the small diameter chiralities that we focus on here. At low added electrolyte concentration, the emission intensity for all s-SWNTs is enhanced (Figure 2b) with the behavior now clearly being observed for smaller-diameter semiconducting chiralities including the (6,5), (8,4), (7,5), and (7,6) species. Further titration results in continued intensity increases for the smaller diameter chiralities, but begins to selectively bleach the emission of large diameter s-SWNTs (note the (11,3), (10,3), (9,8), and (8,7) SWNTs in Figure 2c). The spectra shown in Figure 2d demonstrate that the fluorescence behavior is paralleled in the corresponding absorbance spectra. Both sets of spectra illustrate the spectral narrowing and ~3 nm blue shifting that accompanies enhancement of the features at low-level addition of NaCl. The aggregation threshold becomes apparent with loss of fluorescence intensity and significant broadening of absorbance peaks for the larger diameter species at higher NaCl concentrations. The intensity behavior as a function of NaCl concentration is shown in more detail in Figure 2e for selected s-SWNT chiralities with diameters ranging from 0.757 to 1.05 nm. Intensity enhancement is generalized across all diameters at low NaCl concentrations, but is most pronounced for the smallest diameters. Subsequent loss of emission as the electrolyte concentration increases occurs earlier for large diameter SWNTs.[20] It is apparent from Figure 2e that the magnitude of the (10,5) response is reduced for the 189.2 sample in comparison to that found for the sample used in our previous work.[21] This is a consequence of the shift in diameter distribution to smaller diameter tubes in the current sample (see the Supporting Information). The significantly reduced relative concentration of the (10,5) chirality impacts the SDS equilibrium processes that form the basis for the

(56) Moshammer, K.; Hennrich, F.; Kappes, M. M. *Nano Res.* **2009**, *2*, 599–606.

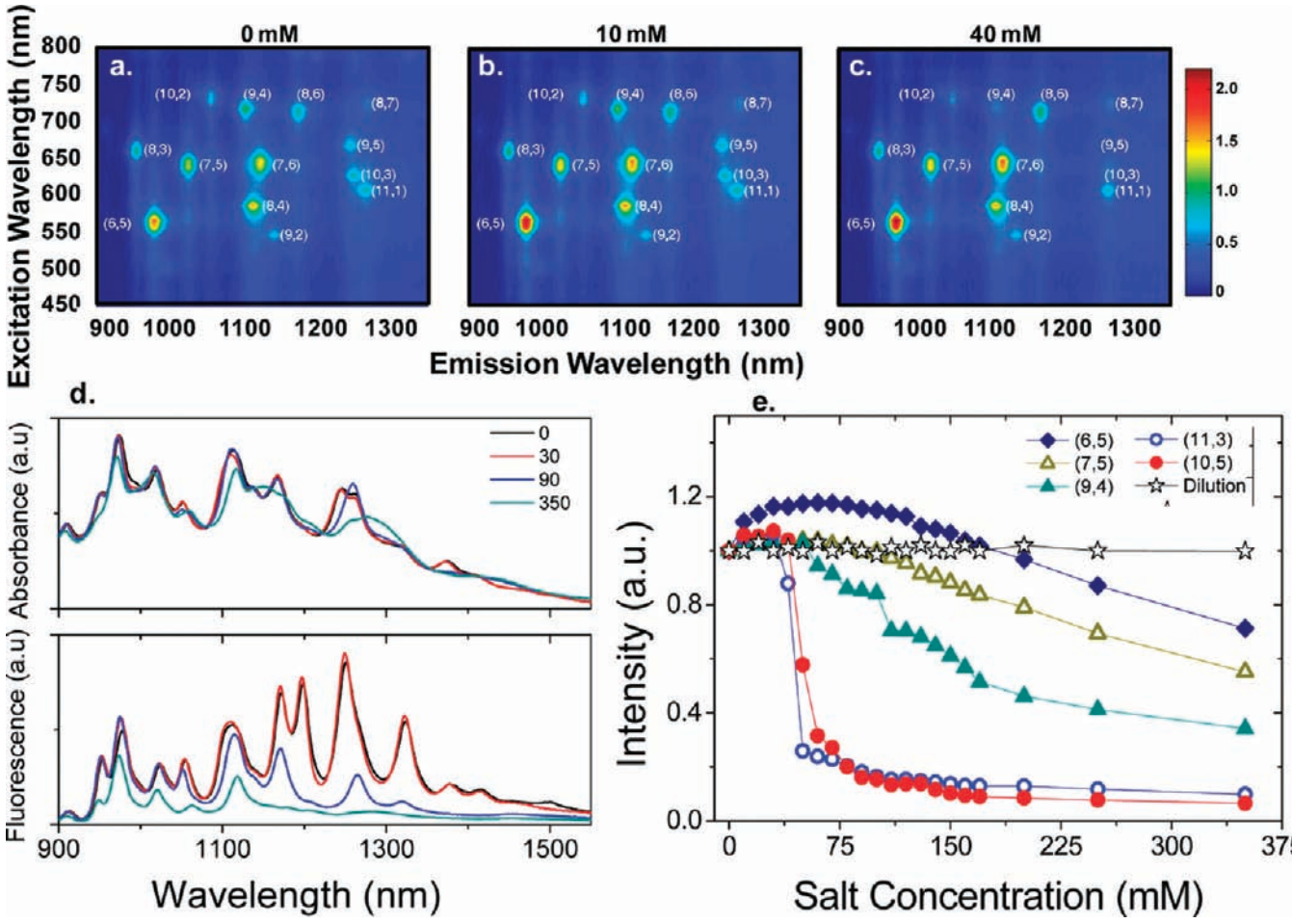

Figure 2. Semiconducting SWNT (s-SWNT) spectral behavior with NaCl addition. (a−c) PL excitation maps (relative intensity scale bar given at right) of 1 wt % SDS−SWNTs (HiPco batch 189.2) after titration to (a) 0 mM, (b) 10 mM, and (c) 40 mM Na^+ with addition of 1 M NaCl solution to 500 μL SDS−SWNT suspensions. s-SWNT (*n*,*m*) identifications for specific PL features are labeled. (d) Absorbance (top) and fluorescence (bottom, 780 nm excitation) spectra of SDS−SWNT suspensions after addition of NaCl solution (black trace, reference; red trace, 30 mM NaCl; blue trace, 90 mM NaCl; and green trace, 350 mM NaCl). (e) Peak emission intensity (at 780 nm excitation) for different (*n*,*m*) SWNTs as a function of salt concentration ((6,5) $d = 0.757$ nm, blue ◆; (7,5) $d = 0.829$ nm, yellow △; (9,4) $d = 0.916$ nm, green ▲; (11,3) $d = 1.014$ nm, blue ○; (10,5) $d = 1.05$ nm, red ●; and ☆, dilution).

behaviors observed in Figure 2. Finally, we note that similar dilution of the SWNT suspensions with D_2O alone (no salt) does not affect the emission intensity throughout the range studied (☆, Figure 2e).

As discussed in earlier work,[21] the observed increase in intensity and spectral narrowing is a consequence of both the increased packing density and the reorientation of the surfactant structure. The result is a reduction in intertube interactions and improved isolation from the local solvent environment reflected in the observed changes in spectral response.[13,21] Relevant to our discussion of saturation of surfactant structure in response to stimuli, the peak found in the PL enhancement as electrolyte concentration is increased corresponds to the point at which surfactant structural saturation occurs.

Given the separations results highlighted in Figure 1, we expect that at sufficiently high SDS concentrations the surfactant structure at the s-SWNT surface will also become significantly altered, with saturation behavior being observed for these species as well. These structural changes should affect the ability of the surfactant to respond to electrolyte additions, as reflected by changes in PL behavior. We therefore probe for these saturation effects by comparing the emission changes of SDS−SWNT suspensions at low and high surfactant concentrations, in response to added electrolyte. Figure 3 shows PL excitation maps for SWNT suspensions in 0.5 and 2.0 wt % SDS, before and after NaCl addition. The bright spectral features in these maps correspond to the excitation/emission maxima of specific s-SWNT structures.[6] At low surfactant concentration (0.5 wt %), a significant enhancement of the emission intensity of all s-SWNT species was obtained after salt addition. In contrast, at high surfactant concentrations, emission intensities remain the same for most species after salt addition. Exceptions are seen for the larger diameter nanotubes, for which loss of intensity is observed, indicating the aggregation threshold is being reached for these species at lower salt concentrations than is found for lower SDS loadings. This observation is consistent with the results shown in Figure 2 and earlier work.[20] These results confirm our expectation that at sufficiently high SDS concentrations its surface structure becomes saturated. Lack of further change in PL response as NaCl is added indicates that a 2% SDS loading induces formation of a stable surface conformation that is no longer able to reorient further in response to electrolyte screening.

The onset of the saturation behavior illustrated in Figure 3 can be better quantified by focusing on the response of selected chiralities over a wider range of electrolyte and surfactant concentration. Figure 4 shows how the integrated emission intensity for (6,5) and (7,6) SWNTs changes with added NaCl

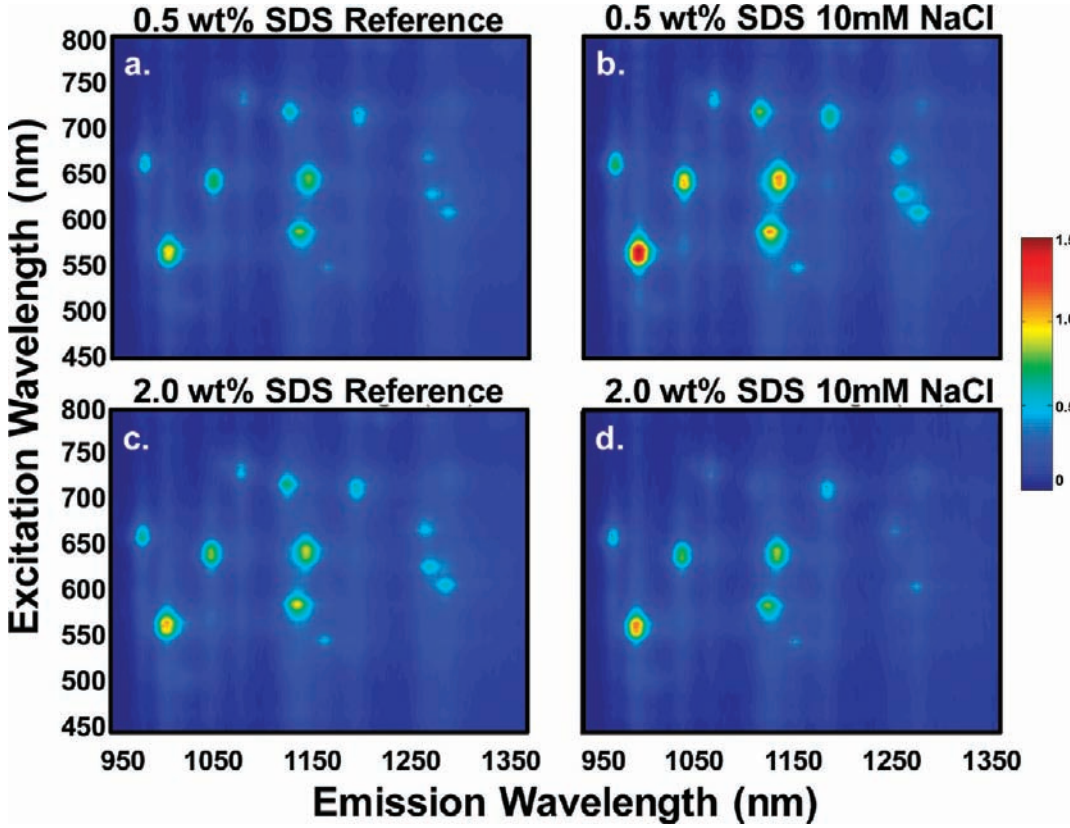

Figure 3. (a−d) PL excitation maps (relative intensity scale bar given at right) of SDS−SWNTs (HiPco batch 189.2) at two different surfactant concentrations (0.5 wt %, (a) and (b); and 2 wt %, (c) and (d)) before and after addition of NaCl to 10 mM final concentration.

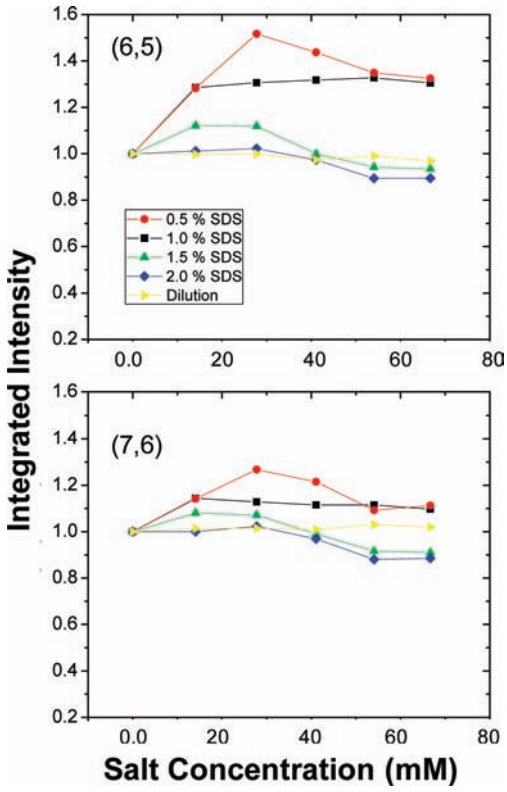

Figure 4. The integrated emission intensity of (a) (6,5) and (b) (7,6) SWNTs as a function of salt (NaCl) concentration at four different surfactant (SDS) concentrations (0.5, red ●; 1.0, ■; 1.5, green ▲; and 2.0 wt %, blue ◆) and D_2O dilution (yellow ▲). Intensities are normalized to that seen for the case of no NaCl addition for each chirality.

at four different surfactant concentrations (0.5, 1.0, 1.5, and 2.0 wt %). The intensities were obtained from spectra excited at resonance with the respective E_{22} transitions (2.191 and 1.914 eV for (6,5) and (7,6), respectively). At low surface coverage, both chiralities show an increase in the emission intensity as initial electrolyte concentrations increase, followed by slight emission decreases at the highest electrolyte concentrations studied. The magnitude of the maximum emission enhancement decreases as the concentration of SDS increases. Finally, at 2% SDS, a loss of sensitivity to salt addition is observed with stable emission intensities over the full range of added electrolyte. We note that dilution of 1 wt % SDS−SWNT suspensions with equal aliquots of 1 wt % SDS−D_2O shows no effect on the emission intensity (yellow trace).

These results indicate that the transition to a saturated surface structure is a continuous process of increased ordering of the SDS conformation and does not result from an abrupt phase change, as was also indicated by the DGU results of Figure 1. Our model of surface reorientation and emission enhancement being driven by an increase in surfactant loading and packing density at the nanotube surface is also further supported.[21] Whether the driving force for increased surface loading is from electrolyte screening or SDS concentration effects, the end result is the same. For both cases, once the SDS surfactant morphology reaches the saturated structure, the PL behavior of s-SWNTs becomes constant. Unsurprisingly, the two effects are also found to be strongly interlinked. Our results clearly demonstrate that increased solution concentrations of SDS directly translate to increased loadings on the nanotube surface as well. The increased surface loading ultimately limits the degree to which

further packing and orientational changes can be induced by electrolyte screening.

These observations also provide important experimental support for several recent molecular dynamics simulations of SDS behavior on SWNTs.[48−52] Each of these reports indicates the occurrence of low surface coverage of uncorrelated structures with SDS chains lying parallel to the SWNT surface at low solution concentrations of SDS. As SDS concentration is increased, a more uniform and densely packed surface structure emerges in the simulations. Moreover, as packing density increases, individual surfactant molecules are found to reorient so that the SDS alkane chains align perpendicular to the SWNT surface and their polar headgroups protrude more directly into the solvent environment, with an accompanying increase in overall volume of the SDS/SWNT composite structure. Expectations from the MD simulations are in direct agreement with our experimental results. Of particular interest are the results of Xu et.al.[52] that suggest the SDS reorientation also results in expulsion of water from the SWNT surface and surfactant structure. Such improved isolation from the solvent environment plus reduction in intertube interactions would directly lead to our observation of the emission enhancement coupled to blue shifting and narrowing of PL spectral features that accompanies the increased packing density and SDS reorientation results.[18,23,32,45]

It is also interesting to note that the overall relative emission enhancement during initial salt titration is greatest for the smallest diameter SWNTs in Figure 4 ($d_{(6,5)} = 0.757$ nm and $d_{(7,6)} = 0.895$ nm). This is also seen over a wider range of nanotube diameters in the data of Figure 2; the smaller diameter chiralities show significantly greater emission enhancements than are observed for larger diameter species. This result also agrees well with the MD simulations, which suggest that a more uniform surface coverage should exist for larger diameter SWNTs.[49,50,52] In the context of the results of Figure 4, at low surfactant concentration the surface coverage is relatively poor for the (6,5) structure in comparison to that of the (7,6). A greater environmental change is therefore experienced by the (6,5) structure on going from such a low coverage regime to the saturated structure that results from NaCl addition. Maximum enhancement of the PL intensity results. Conversely, because larger diameter SWNTs will start with a more uniform and densely packed surfactant coverage, with a greater number of SDS molecules initially oriented perpendicular to the surface, reordering of the surfactant structure will be less upon perturbing the system with electrolyte. Thus, the larger diameter chiralities will display a smaller overall emission enhancement.

Ultimately, the limit of saturation behavior is defined by the aggregation number (N) of the surfactant under specific conditions. In addition to its dependence on surfactant and counterion concentrations (as noted above), N will also depend on the choice of counterion. Changing to one other than Na^+ may define a new saturation limit. Larger cations, like Cs^+ for example, can associate with and bind a greater number of anionic sulfate headgroups. As a result, N in cesium dodecyl sulfate (CsDS) micelles is greater than that for NaDS.[55] Relevant to how behavior at carbon surfaces is affected, recent MD simulations suggest the increased N arising with Cs^+ will more efficiently exclude H_2O from the surface assembly as well.[57]

This expectation is in agreement with our finding that, as aliquots of Cs^+ are added to 1% SDS−SWNT suspensions, PL intensities are enhanced by nearly a factor of 2 (see Figure 5),

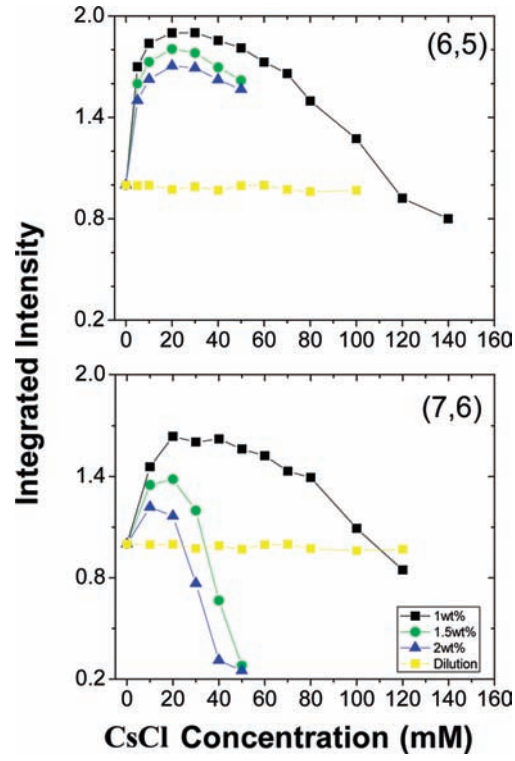

Figure 5. The integrated emission intensity of (a) (6,5) and (b) (7,6) SWNTs as a function of CsCl concentration at three different surfactant (SDS) concentrations (1.0, ■; 1.5, green ●; and 2.0 wt %, blue ▲) and D_2O dilution (yellow ■). Intensities are normalized to that seen for the case of no CsCl addition for each chirality.

indicating greatly reduced H_2O interactions. Furthermore, as found with Na^+ additions, we also observe that the ability of Cs^+ to reorganize the surfactant structure becomes reduced at higher SDS concentrations (Figure 5). However, even at 2% SDS loadings, Cs^+ remains able to perturb the surface structure, with additions still yielding PL intensity increases (although with reduced effect as compared to 1% SDS levels). This behavior can be understood as a result of the increased N available with Cs^+ as compared to Na^+. For example, at 25 mM CsDS (roughly corresponding to the peak of the (6,5) and (7,6) PL response curves in Figure 5), N is on the order of 90, while for 2% SDS, N is approximately 70.[55] Thus, in the presence of Cs^+, SDS−SWNT surface structures can no longer be thought of as saturated.

Dynamics of Reorientation: Surface Access, Surfactant Mobility, and Molecular Structure. Surfactant saturation is a complex process that requires the dynamic mobility of SDS to not only drive more surfactant molecules to the SWNT interface, but also to allow for molecular reorientation once there. Limiting SDS mobility should therefore reduce the dynamic response of the surfactant structure to electrolyte screening effects and in consequence reduce changes in emission intensity, independent of SDS concentration. We investigate this aspect of the saturation phenomena by locking in SDS conformation via coating of the SDS/SWNT structure with a secondary layer of PVP. PVP is well-known to interact strongly with SDS via charge transfer[22,23,58] and to adsorb at the outer SDS micelle.[23] As a result, the PVP−SDS interaction inhibits the SDS mobility and should prevent surfactant reorganization during salt titration.

(57) Tummala, N. R.; Striolo, A. *J. Phys. Chem. B* **2008**, *112*, 1987–2000.

(58) Zhai, L.; Lu, X.; Chen, W.; Hu, C.; Zheng, L. *Colloids Surf., A* **2004**, *236*, 1–5.

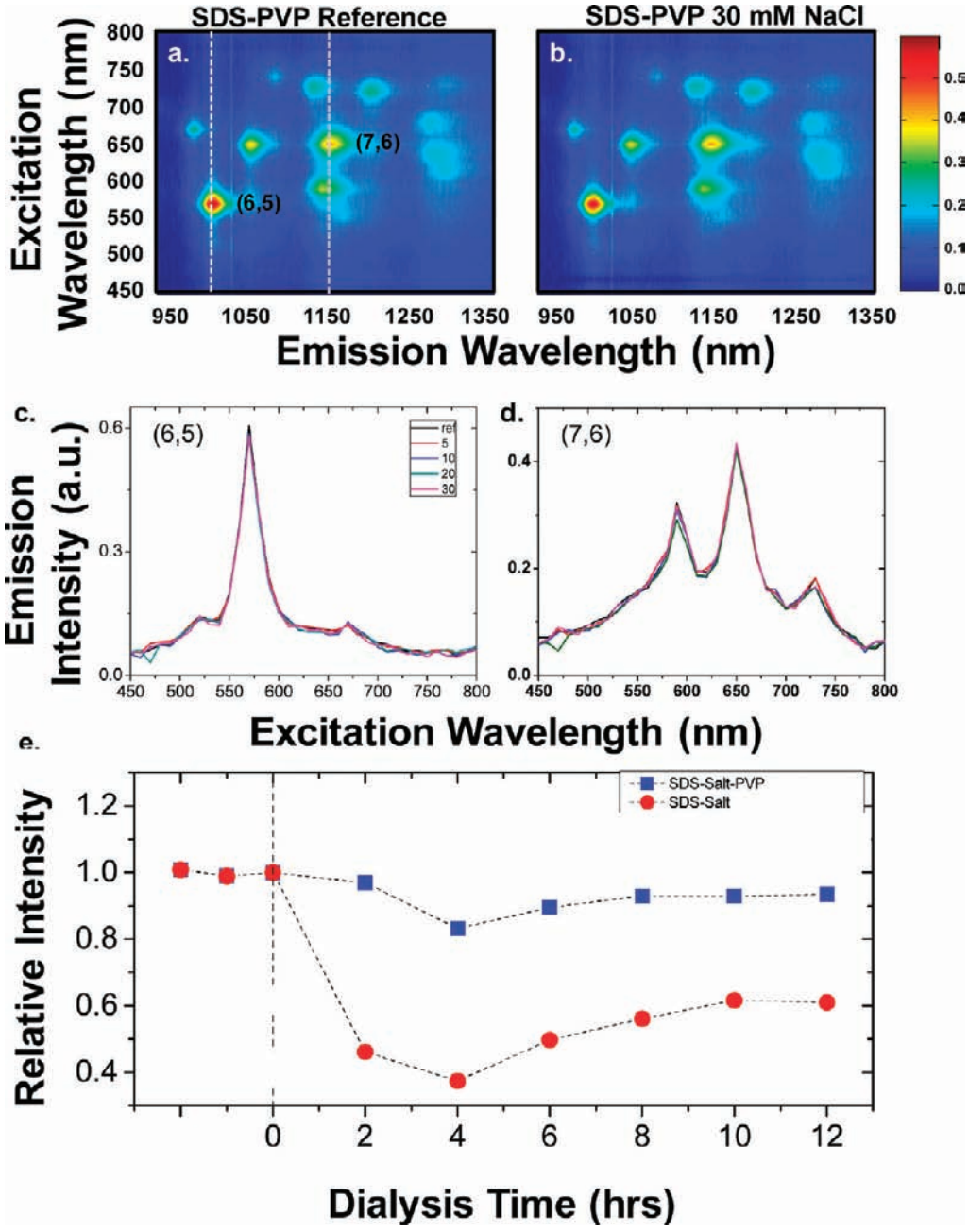

Figure 6. (a,b) PL excitation maps (intensity scale bar at right) of SDS−PVP−SWNT suspensions before (a) and after (b) salt titration (to 30 mM NaCl). (c,d) Emission intensity as a function of excitation wavelength for PVP−SDS−SWNT suspensions after salt titration (reference, black trace; 5 mM NaCl, red trace; 10 mM NaCl, blue trace; 20 mM NaCl, green trace; and 30 mM NaCl, pink trace) for the (6,5) and (7,6) SWNTs, respectively. Dotted lines in (a) correspond to the emission wavelength used to generate (c) and (d). (e) Relative (6,5) PL intensity (normalized to peak intensity at time 0) for two SWNT suspensions dialyzed against 0.75% SDS−SWNT. Red ●: 0.75% SDS-SWNT in 30 mM Na^+. Blue ■: 0.75% SDS−SWNT prepared in 30 mM Na^+ followed by stabilization with PVP.

Moreover, the PVP layer will block exchange of large molecules, while being permeable to small ionic species such as Na^+.[23] We observed that addition of PVP to the SDS suspension results in PL spectra that are red-shifted, broadened, and reduced in intensity for all SWNT types (relative to the initial SDS suspension), indicating a strong interaction between the surfactant and the polymer.[23] Figure 6 shows PL excitation maps of SDS−PVP suspensions (∼0.75% final SDS concentration) before (Figure 6a) and after (Figure 6b) addition of NaCl. We find that the intensity, peak location, and line-width of the SWNT emission remained constant after salt titration for all SWNT chiralities. Emission intensity for the (6,5) and (7,5) SWNTs (Figure 6c and d) is found to remain stable over a range of NaCl concentrations that would otherwise enhance the PL emission in the absence of PVP. Even at very high salt concentrations (>100 mM), we did not observe any emission changes or signs of aggregation. These observations are also consistent with the previously observed emission stability of the SDS−PVP−SWNT system in biological media with high salt concentrations like phosphate buffered saline.[23] Such remarkable stability in the presence of strong electrolyte screening demonstrates that PVP is able to lock in the surface conformation of the surfactant and inhibit its reorganization. A significant component of the orientation stability is also due to PVP preventing further migration of SDS from the bulk solution into the SWNT surface structures. Hence, no photophysical

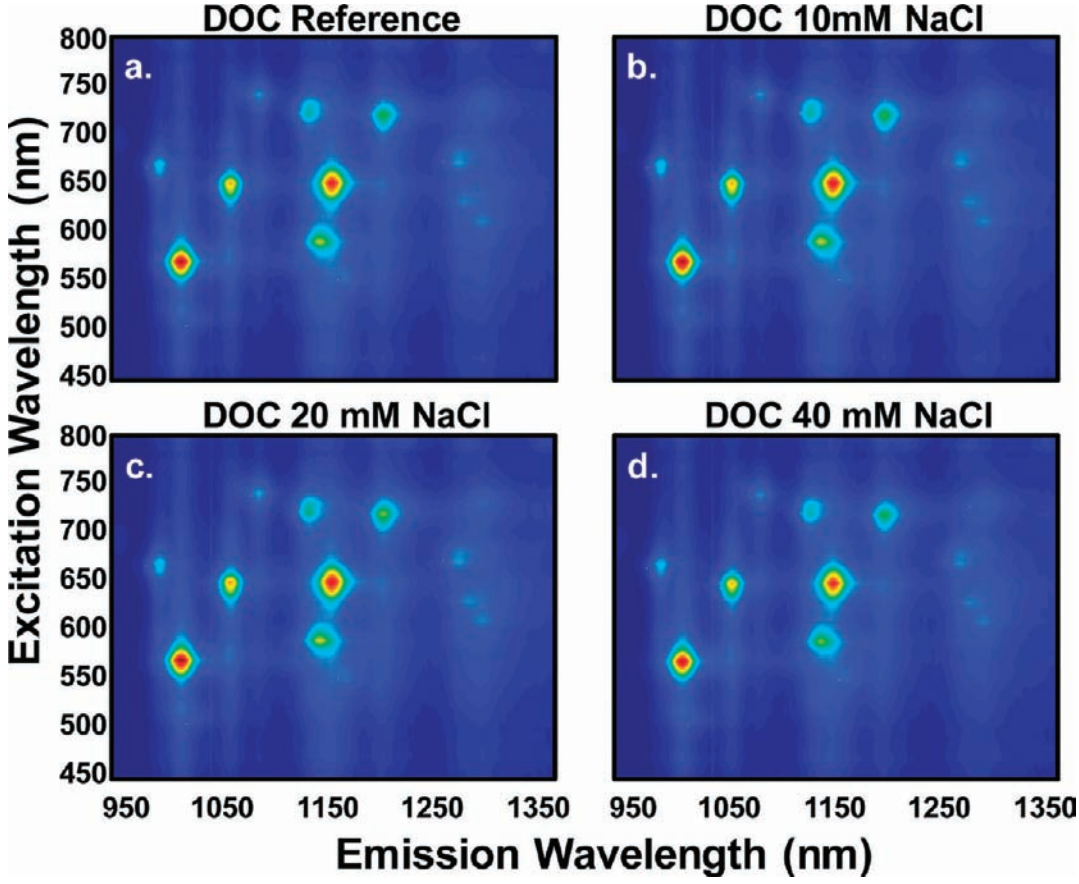

Figure 7. (a−d) PL excitation maps of DOC−SWNT suspensions after salt titration. (a) Reference, (b) 10 mM NaCl, (c) 20 mM NaCl, and (d) 40 mM NaCl.

changes are observed in SDS−PVP−SWNT suspensions after salt titration.

SDS mobility can also potentially lead to reversal of saturated structures. We therefore study the reverse case in which Na^+ is first used to induce a SDS conformational change that maximizes PL intensity. With this saturated SDS starting geometry, we explore if subsequent PVP addition is able to prevent relaxation of the SDS conformation to a less ordered and thus more weakly emitting structure. A 0.75% SDS−SWNT suspension is brought to 30 mM in Na^+, resulting in the expected ∼50% increase in PL intensity resulting from generation of the saturated surface structures. A portion of this sample is stabilized by PVP addition as described above. The unstabilized sample is dialyzed against a 0.75% SDS solution so that Na^+ is removed, while the SDS concentration of the SWNT suspension remains constant. As seen in Figure 6e, as Na^+ is removed, PL intensity is lost until the original intensity in the absence of Na^+ is reached. Importantly, this result demonstrates that saturation of the surfactant structure can be reversed in the absence of other stabilizing interactions. In contrast, Figure 6e shows that the PVP-stabilized sample shows only limited loss in PL intensity under identical dialysis conditions. Thus, we demonstrate that limiting the ability of SDS to reorient can also be used as a route to stabilizing the saturated surfactant structures.

Surfactant mobility and its ability to reorient in response to external forces will also be significantly impacted by specific interactions with the SWNT surface as defined by the surfactant molecular structure. SDS has a long flexible and dynamic hydrocarbon chain, which gives fewer initial constraints on its orientation upon adsorption (via relatively weak hydrophobic interactions) to the SWNT surface. SDS is therefore able to respond freely to an external organizing force through conformational changes.[19,21,26] In contrast, the large planar ring structures of bile salts like deoxy cholate (DOC) or sodium cholate (SC) have a more constrained geometry and a stronger interaction with the SWNT surface, even below their critical micelle concentrations after extended dialysis.[16] Furthermore, recent diameter-dependent DGU separations of SWNTs with bile salts indicate a possible registry with the SWNT structure[38,59,60] that also provides better isolation from local environments.[15,18] Given these differences in structural flexibility and interaction characteristics that ultimately impact observed photophysical properties and separations behavior, it is important to determine if the range of structural reorganization accessible to SDS is general to more strongly interacting surfactants like the bile salts.

To evaluate the susceptibility of bile salt interactions with the nanotube surface to conformational changes induced by electrolyte addition, SWNT suspensions in 1 wt % DOC were monitored for optical changes upon titration with NaCl. Figure 7 shows PL excitation maps of a DOC−SWNT suspension titrated to 40 mM NaCl. The SWNT optical properties remain constant (i.e., no peak shifts, spectral broadening, or intensity changes) across the full titration range, indicating that electrostatic screening does not change the surfactant conformation around the SWNTs. Similar results were found with SDBS (see

(59) Zhao, P.; Einarsson, E.; Xiang, R.; Murakami, Y.; Maruyama, S. *J. Phys. Chem. C* **2010**, *114*, 4831–4834.
(60) Haroz, E. H.; Rice, W. D.; Lu, B. Y.; Ghosh, S.; Hauge, R. H.; Weisman, R. B.; Doorn, S. K.; Kono, J. *ACS Nano* **2010**, *4*, 1955–1962.

Supporting Information Figure S.2), which has similarly strong interactions with the SWNT surface. These observations can be explained by the strong specific interactions between the SWNT surface and these surfactants. For DOC, these result in a more complete close-packed coating of the nanotube surface that is also limited in its ability to reorient in response to screening and other forces.

These results have important implications for enhancing DGU-based separations via similar effects. Effects on cosurfactant systems involving SDS are likely to act through the tunability of the SDS structures, while DOC interactions are likely to be unaffected. Consistent with this expectation, it is important to note that we do not observe SWNT fractionation in a DGU separation when DOC is used as the sole surfactant in the presence of added salt. The contrasting behaviors of SDS and DOC under the influence of reorganizational forces such as electrolyte screening and change in surfactant concentration have important implications for further enhancing DGU-based separations. The impact of such effects in cosurfactant systems is likely to act through the tunability of SDS structures, while the DOC−SWNT interactions are likely to remain unaffected.

This picture supports a recent model (DOC restriction of SDS wrapping) used to explain a highly successful DGU expansion of s-SWNTs into well-resolved fractions of various narrow diameter distributions using a SDS/DOC cosurfactant system.[59] In the model of Zhao et al.,[59] SDS is thought to adsorb to the SWNT surface left available due to incomplete coverage by DOC. DOC is suggested to pack less densely on small diameter SWNTs than on larger diameter species, making more surface area available to SDS on the former. Smaller diameter nanotubes thus move to the lower density fractions in DGU. Furthermore, Zhao et al. find that spatial separation of their fractions increases significantly when working at higher SDS concentrations, with the smallest diameter species experiencing the greatest change in density. This result is in excellent agreement with our picture of surfactant saturation. Increasing SDS concentrations will force more surfactant to the available adsorption sites, driving surface reorientation most effectively on the small diameter SWNTs. Small diameter SWNTs should therefore experience the greatest shift to lower density. The larger diameter SWNTs, with less surface available for new SDS binding, will reach saturation first. Their density response will therefore be much less affected, in agreement with the results of ref 59.

Conclusion

Surfactant structure at the SWNT surface is demonstrated to be a dynamically tunable system with significant ability to reorganize within broad limits as electrostatic and concentration influences are changed. Saturation in the dynamic response to such influences can result from a number of sources, including the interactions of the surfactant molecules with themselves as packing density is optimized, interactions with the secondary molecular structure that surrounds the surfactant−SWNT composite assembly, and the direct interactions with the SWNT surface. These are further influenced by the underlying nanotube structure, with SWNT metallicity being shown to be especially important. Saturation in the ability of surfactant structure to reorganize is thus demonstrated for both metallic and semiconducting SWNTs. The diameter dependence in such saturation behavior further adds to our understanding of how surfactant reorganizational behavior influences the diameter dependence of density-based separations. The results provide an additional guide toward surfactant engineering for enhancing separations and tuning optical parameters for sensing, imaging, and nanophotonics applications. Our results represent important confirmation of several models for surfactant behavior and will be a useful reference point for refining the accuracy and detail of MD simulations that are beginning to show potential for predictive capability. Simulations of metallicity effects, however, remain a compelling challenge. Developing new approaches to probing the surface behaviors of low-dimensional nanomaterials in general will continue to be of growing importance. Our demonstrated methods of perturbing surfactant structure followed by probing SWNT optical and density response may be further extended by applying alternative reorganizing forces including mechanical and chemical influences and following surfactant response with time-dependent spectroscopies. These techniques will continue to be effective probes of new behaviors in both pure and mixed surfactant systems.

Acknowledgment. We thank the Smalley Institute for Nanoscale Science and Technology at Rice University for supplying SWNTs. This work was supported by LANL-LDRD funding. J.G.D. thanks the LANL-LDRD Director's Postdoctoral Fellowship. This work was performed in part at the Center for Integrated Nanotechnologies, a U.S. Department of Energy, Office of Basic Energy Sciences user facility.

Supporting Information Available: Additional figures. This material is available free of charge via the Internet at http://pubs.acs.org.

JA106836F